Separation and Purification Technology 122 (2014) 159–169

Contents lists available at ScienceDirect

Separation and Purification Technology

journal homepage: www.elsevier.com/locate/seppur

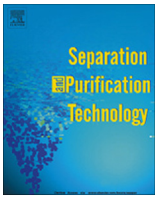

Transcolumn dispersion in a computational mimic of an analytical silica monolith reconstructed from sub-microtomographic scans using computational fluid dynamics

Vivek Vasudevan, Kai-Chee Loh [*]

Department of Chemical and Biomolecular Engineering, National University of Singapore, 4 Engineering Drive 4, Singapore 117585, Singapore

ARTICLE INFO

Article history:
Received 24 January 2013
Received in revised form 28 October 2013
Accepted 31 October 2013
Available online 14 November 2013

Keywords:
Computed tomography
Computational fluid dynamics
Silica monolith
Transcolumn dispersion
Phenomenological approach

ABSTRACT

Analysis of transcolumn dispersion in an analytical silica monolith is presented via direct numerical simulations in a topological model reconstructed from 3D nanotomographic scans. This was the first instance to incorporate retention in the study of dispersion behavior in reconstructed models for monoliths. The low scanning resolution employed in this work allowed simulating retained behavior with no appreciable loss of prediction accuracy. Heterogeneities of the order of 1–2 domain lengths were observed from peak parking and transient dispersion simulations, indicating a relatively homogeneous core in silica monoliths. Analysis of the short-range interchannel dispersion revealed that equilibration at the domain-level occurred mainly through lateral diffusion. Phenomena not captured by the model, viz. transcolumn eddy dispersion and dispersion due to external film mass transfer resistance, were estimated from deviations of simulated data from experimental values. Three scenarios were explored to model the transcolumn and external film mass transfer resistance contributions to overall dispersion. In the first case, when transcolumn dispersion was controlled by a convection mechanism, the transcolumn velocity biases were within the experimentally observed ranges for silica monoliths. Deviations of estimated film mass transfer resistance from that predicted by penetration theory varied inversely with the zone-retention factor. In the second case, when film penetration theory was assumed to hold good and the transcolumn contribution was modeled to exhibit a coupled diffusive-convective behavior, the corresponding persistence-of-velocity lengths revealed that about 20–30% of the column length was utilized in relaxing the transcolumn concentration gradients. A phenomenological approach was proposed to estimate transcolumn dispersion from the simulated transverse dispersion coefficients and column residence times. The parameters estimated from the proposed approach were compared with the third scenario, wherein transcolumn dispersion was modeled according to Giddings' couple equation, while external film mass transfer resistance was assumed to deviate from film penetration theory. In the absence of any method to predict a priori or directly measure transcolumn dispersion and external film mass transfer resistance in silica monoliths, this approach served as a first approximation to judge the magnitude of each contribution to overall dispersion.

1. Introduction

Silica monoliths are essentially used for conventional RPLC separations and analyses of small or medium molecular weight range compounds, typical of those analyzed in the fine chemical, agricultural, food, and classical pharmaceutical industries [1]. The regular structural network of macropore channels, less constricted and less tortuous than in packed beds, results in a high external porosity [2]. The stationary phase skeleton, made of a network of small, thin threads of porous silica, has no effect on hydraulic resistance and hence, can be reduced to accelerate the mass transfer of sample molecules. These structural characteristics provide a combination of low hydraulic resistance to the mobile phase, and enhanced mass transfer rates of sample molecules through the silica monolith. However, the first generation silica monoliths did not achieve the successful commercialization that was originally expected [1]. Structural features, inherent to their fabrication process, made the silica monoliths radially heterogeneous [3,4].

The eddy diffusion A-term in the van Deemter equation was recognized to limit the efficiency of silica monoliths [1,5]. Monolithic columns would have a lower eddy diffusion term and be more efficient than packed columns if they did not suffer from an intrinsic and undesired radial structural heterogeneity that arises due to shrinkage of silica during the sol–gel preparation process [1,3,4]. This radial heterogeneity, though nearly impossible to

---

[*] Corresponding author. Tel.: +65 65162174; fax: +65 67791936.
E-mail address: chelohkc@nus.edu.sg (K.-C. Loh).

1383-5866/$ - see front matter © 2013 Elsevier B.V. All rights reserved.
http://dx.doi.org/10.1016/j.seppur.2013.10.050

Nomenclature

C	bulk mobile phase mass fraction of *phenol*
C_i	mass fraction of analyte at *i*th detection plane
C_s	effective (volume-averaged) mass fraction of *phenol* in porous skeleton
C_s^*	mass fraction of adsorbed species *phenol**
d_{dom}	domain-length, μm
D_{eff}	effective diffusivity of species *phenol* in chromatographic bed, m^2/s
$D_L(t)$	transient axial dispersion coefficient, m^2/s
D_m	diffusion coefficient in bulk mobile phase, m^2/s
D_{skel}	effective diffusion coefficient in porous skeleton, m^2/s
d_{skel}	size (diameter) of porous skeleton, μm
$D_T(t)$	transient transverse dispersion coefficient, m^2/s
h_{Film}	reduced-HETP contribution due to external film mass transfer resistance
$h_{Long.}$	contribution to overall reduced-HETP due to axial diffusion
$h_{S\text{-}Rinterchannel}$	reduced-HETP contribution due to short-range interchannel eddy dispersion
$h_{Skel.}$	reduced-HETP contribution due to stationary-phase mass transfer resistance
h_{expt}	reduced-HETP calculated from experiments
h_{sim}	reduced-HETP calculated from axial dispersion simulations
$h_{transchannel}$	reduced-HETP contribution due to transchannel eddy dispersion
$h_{transcolumn}$	reduced-HETP contribution due to transcolumn dispersion
$H(t)$	transient HETP
k''	zone retention factor
K	equilibrium constant
k'	phase retention factor
k''_0	zone retention factor under non-retained/porous conditions
k_b	desorption rate constant, s^{-1}
k_f	adsorption rate constant, s^{-1}
L	length of column, cm
M_A	molecular weight of water, g/mol
M_B	molecular weight of methanol, g/mol
phenol	freely diffusing species in bulk/porous skeleton
*phenol**	adsorbed species in porous skeleton
R_s	rate of formation of species in porous skeleton, s^{-1}
$t_{R,ex}$	extra-column elution time of chromatogram at its apex, s
$t_{R,i}$	retention time of analyte at *i*th detection plane, s
t_R	elution time of chromatogram at its apex, s
$t_{f,1/2,ex}$	extra-column elution time of chromatogram at half-height during adsorption, s
$t_{f,1/2}$	elution time of chromatogram at half-height during adsorption, s
$t_{r,1/2,ex}$	extra-column elution time of chromatogram at half-height during desorption, s
$t_{r,1/2}$	elution time of chromatogram at half-height during desorption, s
T	temperature, K
u_{ave}	average interstitial velocity, m/s
u_{sf}	superficial velocity, m/s
V_b	molar volume of analyte (phenol) at its boiling point, cm^3/mol
x_A	molar fraction of water
x_B	molar fraction of methanol
$\bar{z}$	mean spatial location of species distribution in macropore space

Greek symbols

α	deviation of estimated film resistance from that predicted by penetration theory
γ_e	external obstruction factor
ε_e	external porosity of silica monolith
ε_{int}	internal porosity of porous skeleton (=0.5)
ε_t	total porosity of silica monolith
μ_{AB}	viscosity of mobile phase, cP
ν_{ave}	reduced-linear velocity or Peclet number
σ_z^2	spatial variance of species distribution
φ_A	associative factor for water
φ_B	associative factor for methanol
ω_α	non-dimensionalized lateral diffusion distance
ω_β	transcolumn velocity bias
ω_λ	non-dimensionalized persistence-of-velocity length
Ω	ratio of effective diffusivity through porous skeleton to bulk diffusivity

assess from SEM images, was experimentally observed by local electrochemical detection at various radial positions of the outlet cross-sectional area of a silica monolith [3]. The relative velocity difference between the center and the wall of commercial analytical silica monoliths was about 2% [4].

Eddy dispersion arises from band spreading caused by velocity biases within the chromatographic column. This band broadening, accounted for in the overall band dispersion by the coupling theory of eddy dispersion by Giddings [6], was expressed as a sum of four contributions that described the erratic mass transfer by flow and diffusion on different length scales: (i) transchannel, (ii) short-range interchannel, (iii) long-range interchannel, and (iv) transcolumn. Typically in packed columns, at high linear velocities, 45% of the eddy dispersion was accounted by transchannel velocity bias, 45% by short-range interchannel velocity bias and 10% by long-range interchannel velocity bias. The transcolumn velocity bias was severe only under non-adiabatic conditions where a radial temperature gradient increased the degree of radial heterogeneity [7,8]. Transcolumn dispersion, however, was suspected to be the primary cause of inefficiency in the first generation of silica monoliths ever since they were commercially available in the early 2000s [9].

Transcolumn dispersion accounted for about 75% of the total eddy dispersion in silica monoliths [9]. It arises due to the inability of analyte molecule to sample the entire cross sectional area before leaving the monolithic column due to the relative difference in the linear velocities between the column center and wall. Monolithic columns generally showed smaller radial dispersion coefficients due to relatively less abrupt changes in streamline directions than in packed beds [10]. These resulted in slower radial mixing, and hence required a longer time for radial concentration gradients to be relaxed, yielding a higher transcolumn dispersion.

Recent advances in non-invasive imaging and high speed computation have made it possible to visualize the macropore morphology in monoliths [11–18]. The transcolumn dispersion was estimated in a 100 μm I.D. bare-silica Chromolith capillary CapRod™ from CLSM reconstructions and was noted to be different from that observed in analytical silica monoliths [15]. Gritti and Guiochon [5,9] developed an experimental protocol to estimate the transcolumn dispersion in analytical silica monoliths from an